

Investigation of the superconducting state of ternary molybdenum sulfides

N. E. Alekseevskii, A. V. Mitin, and E. P. Khlybov

Institute of Physics Problems, USSR Academy of Sciences

(Submitted 23 October 1981)

Zh. Eksp. Teor. Fiz. **82**, 927-940 (March 1982)

The properties of the superconducting state of bulk samples of ternary molybdenum sulfides containing copper, tin, and lead were investigated. The highest values of all three critical parameters T_c , H_{c2} , and J_c were observed in compounds with lead. Variation of the annealing temperature from 720 to 1120° C at one and the same annealing time (24 h) leads to a change in the density of the critical current in $Pb_{1.2}Mo_{6.4}S_8$ samples by more than one order of magnitude, whereas the remaining critical parameters undergo changes in the range of 40%. The maximum critical-current density $J_c(140 \text{ kOe}; 1.7 \text{ K}) = 3.5 \times 10^8 \text{ A/m}^2$ is reached at an annealing temperature 920° C. The connection between the shapes of the $J_c(H, T = \text{const})$ curves and the damping rate of the critical current in hollow cylindrical samples is analyzed.

PACS numbers: 74.70.Lp, 74.40. + k, 81.40.Rs

INTRODUCTION

Ternary molybdenum chalcogenides $A_xMo_6X_8$ (A -metal, X -chalcogen) have been among the most thoroughly investigated numerous compounds synthesized in recent years. The increased interest in these systems is due both to the unusually broad spectrum of the physical properties and to the fact that they include superconductors with record second-critical-field values $H_{c2} > 500 \text{ kOe}$.¹⁻³

Depending on the ion radius of the element A and its location in the crystal lattice relative to the inversion center $(0, 0, 0)$, ternary molybdenum chalcogenides are divided into two groups.⁴ The compounds of the first group, which are characterized by a rhombohedral angle $\alpha_R > 90^\circ$, have the A cations shifted relative to the inversion center, whereas the compounds of the second group ($\alpha_R < 90^\circ$) have the larger-radius A cations localized near $(0, 0, 0)$.

From among the first group, the superconductor with the highest temperature ($T_c = 11 \text{ K}$) is the compound $Cu_{1.8}Mo_6S_8$. Among the compounds of the second group, the maximum values, $T_c = 14-15 \text{ K}$, are possessed by molybdenum sulfides with lead, whose second critical field $H_c(T = 0)$ is three or four times larger than that of $Cu_{1.8}Mo_6S_8$.

Besides the extremely high values of H_{c2} , ternary molybdenum sulfides with lead have, as first demonstrated in Refs. 5 and 6, also sufficiently high densities of the critical current J_c . The high current-carrying capacity served not only as an additional stimulus for the study of the properties of the superconducting state of ternary molybdenum sulfides, but also uncovered prospects of their practical utilization.

The measurements of J_c were made both on thin-layer coatings^{5, 8-14} and on bulk samples.^{6, 7, 15, 16} The electric-current density in a field of 80 kOe at $T = 4.2 \text{ K}$, for different samples, ranged from 5×10^6 to $2 \times 10^5 \text{ A/m}^2$. So large a scatter in the value of J_c could be attributed to the presence of microcracks, to the influence of the contacts, and to a strong dependence of the quality of the sample on the composition and on the preparation con-

ditions. Thus, e.g., in Ref. 6 and 7 it was shown that in bulky $SnMo_6S_8$ and $PbMo_6S_8$ J_c first increases, with increasing compression prior to annealing and with increasing annealing time, and then saturated. An increase of x from 1 to 1.5 in the $Pb_xMo_{6.3}S_8$ system leads, as shown earlier,¹⁶ to an almost threefold increase of J_c in the entire magnetic-field interval, whereas the remaining critical parameters change in this case by not more than 20%. Since many properties, particularly the microstructure of the samples, depend on the heat treatment, it was of interest to ascertain the influence exerted by the annealing temperature on the critical parameters of ternary molybdenum sulfides.

The use of bulk samples makes it possible to monitor the composition and the manufacturing conditions more accurately than in the case of thin-film coatings. In addition, it is convenient to measure J_c in such samples by contactless methods,^{17, 18} so that it is possible to plot the temperature dependences of J_c from 4.2 K to T_c , where the errors of the contact methods can be particularly large.

We report here the results of investigations of the properties of bulky polycrystalline $Cu_{1.8}Mo_6S_8$, $Sn_{1.2}Mo_{6.4}S_8$, and $Pb_{1.2}Mo_{6.4}S_8$ in the superconducting and normal states, carried out in a single technological regime, and present data on the influence of the annealing temperature on the critical parameters of the $Pb_{1.2}Mo_{6.4}S_8$ system.

EXPERIMENT

Directly synthesized powders on the initial $Pb_{1.2}Mo_{6.4}S_8$, $Sn_{1.2}Mo_{6.4}S_8$, and $Cu_{1.8}Mo_6S_8$ were thoroughly ground in an agate mortar and pressed in cylindrical matrices at pressures 15-20 kbar. The compressed samples, of 2 g mass, were sealed in quartz ampoules filled with pure helium at pressure 0.2-0.25 bar, and subjected to homogenizing annealing at a temperature 920-930° C for 24 h. In a number of cases, such as for the $Pb_{1.2}Mo_{6.4}S_8$ samples, the annealing was at various temperatures, ranging from 720 to 1120° C. The annealing time was in this case 24 h.

TABLE I. Parameters of crystal lattice and resistivity of ternary molybdenum sulfides.

Sample No.	Composition	T_a , °C	α_R	a_R , Å	a_H , Å	c_H , Å	V_H , Å ³	ρ_n , 10 ⁻⁹ Ω · cm	ρ_{300}^{100n}
1	Pb _{1.2} Mo _{6.4} S ₈	720	89.44	6.54	9.20	11.43	838	6700	3.69
2		820	89.39	6.54	9.20	11.45	839	430	2.54
3		920	89.40	6.545	9.207	11.454	840.9	230	2.16
4		1020	89.41	6.538	9.199	11.441	838.5	370	1.93
5		1120	89.41	6.541	9.203	11.445	839.5	610	1.76
6	Sb _{1.2} Mo _{6.4} S ₈	920	89.66	6.516	9.188	11.354	830.1	420	2.23
7	Cu _{1.2} Mo _{6.4} S ₈	920	94.98	6.507	9.594	10.245	816.8	120	11

As a rule, the annealed samples were strong enough and had no visible defects such as cracks, pores, etc. When necessary, the correct sample shape could be obtained by mechanical working.

The phase composition and the parameters of the crystal lattice of the samples were determined with a "Geigerflex" diffractometer (CuK α radiation, $\lambda = 1.541$ Å). The internal standard was silicon powder. The reflections of the samples annealed at low temperatures $700 < T_a < 900$ °C were smeared out and the accuracy in the determination of the hexagonal-cell parameters a_H and c_H was 0.008 Å. For samples with higher annealing temperatures $T_a > 900$ °C, the reflections became more distinct, and the accuracy of a_H and c_H was correspondingly improved to 0.003 Å. The crystallographic parameters for the lowest-temperature ternary molybdenum sulfides with lead, tin, and copper are listed in Table I.

Figure 1 shows the phase-content diagram as a function of the annealing temperature T_a for the system Pb_{1.2}Mo_{6.4}S₈, plotted from x-ray diffraction analysis data. The diagram is approximate, since an exact determination of the phase content is difficult. For comparison, the left-side of the figure shows the relative content of the initial components in the charge.

The values of $H_{c2}(T)$ and $T_c(H=0)$ were determined by a four-contact potentiometer method and corresponded to the midpoint of the transition curve. The current density in the sample during the course of such measurements of $H_{c2}(T)$ and T_c was maintained constant at 1 A/cm². Stationary magnetic fields of intensity up to 150 kOe were produced by water-cooled solenoids of the Bitter type at the International Laboratory For Strong Magnetic Fields And Low Temperatures (Wroclaw, Po-

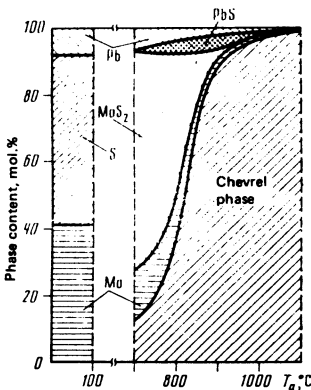


FIG. 1. Phase-content diagram as a function of the annealing temperature T_a for the system Pb_{1.2}Mo_{6.4}S₈.

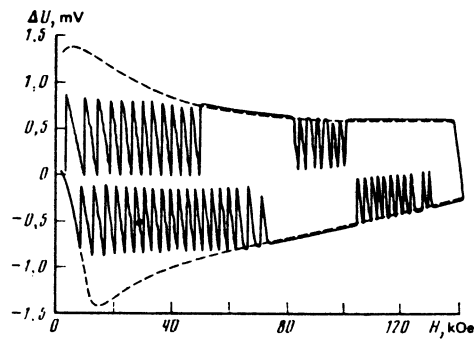


FIG. 2. Hysteresis curves for a Pb_{1.2}Mo_{6.4}S₈ sample with $T_a = 1120$ °C, plotted at $T = 3$ K at different magnetic-field scanning rates 10^2 Oe/sec (dashed line) and 10^3 Oe/sec (solid line).

land). The measurements were made in helium-3, in the temperature range 0.5–1.7 K and in helium-4 at higher temperatures. The sample temperature was monitored during the measurements with carbon thermometers whose readings in the magnetic field were corrected in analogy with the procedure used in Ref. 19.

The critical current density $J_c(H)$ at a fixed temperature was determined by a contactless method, by observing the penetration of the magnetic field into a hollow cylindrical sample whose axis was parallel to the magnetic field. The samples used in the experiments had an outside diameter 5 mm, a height 20 mm, and a wall thickness 1.2–1.5 mm. The difference between the field inside and outside the sample,¹⁾ produced by the currents circulating in the sample, was measured by two calibrated copper pickups, one placed at the center of the cylindrical cavity of the sample, and the other 1 cm away in the plane perpendicular to the field. The pickups were connected in a bridge circuit, whose unbalance signal, proportional to the differences ΔH , was fed to the Y input of an X-Y recorder, while the X input received a signal proportional to the applied magnetic field H . At a specified sample temperature, which was maintained constant with a regulator, the magnetic-field scan was turned on and the plotter traced a hysteresis curve. Figure 2 shows two such curves plotted at $T = 3$ K for sample No. 5. One of the curves, shown dashed, corresponds to a field scanning rate $\partial H / \partial t \approx 10^2$ Oe/sec. At a higher scanning rate $\partial H / \partial t \approx 10^3$ Oe/sec the change of the field in the sample, as seen from Fig. 2, is accompanied by jumps in the flux. A comparison of the data obtained for the molybdenum-sulfide samples of the first and second groups allow us to conclude that the jump probability is proportional to the field scanning rate $\partial H / \partial t$, to the derivative $\partial J_c / \partial H$, and to the field gradient $\partial H / \partial r$ in the sample. The probabilities of the flux jumps at a fixed scanning rate increases as a rule also with decreasing temperature.

The heat released during the time of the flux jumps leads to an abrupt rise in the sample temperature, followed by an exponential decrease whose relaxation time depends mainly on the conditions of the heat exchange between the sample and the coolant. When the measurements are made in the facility with helium-3, which

has relatively low cooling ability, at low temperatures ($T < 0.6$ K), the characteristic relaxation time can reach several minutes. On the other hand if the sample is cooled by a sufficient amount of liquid or gaseous helium-4 (at $T > 4.2$ K), the relaxation time decreases to fractions of a second.

It is seen from Fig. 2 that with decreasing rate of the field scanning from 10^3 to 10^2 Oe/sec, the unbalance signal ΔU from the pickup becomes 3–4% smaller on those sections of the $\Delta U(H)$ curves where there are no flux jumps. The influence of the field scanning rate on the internal field H_i in the sample leads to the conclusion that H_i decreases with time. The change of H_i at given values of the external field $H = \text{const}$ and of the sample temperature $T = \text{const}$ was read at definite time intervals with a digital voltmeter accurate to 0.02–0.005%. The $H_i(t)$ dependences were plotted at several values of the temperature in the range from 1.7 to 4.2 K, and in a number of cases also at $T = 0.5$ K. During such experiments, which lasted several hours each, the sample temperature was maintained accurate to 0.01–0.03 K, while the external field was as a rule turned off. This eliminated automatically all the errors due to the instability of the field H in the Bitter solenoid, and furthermore increased the measurement accuracy because of the simultaneous increase of the difference $\Delta H_i = H_i - H$ and the relative rate of change of the field trapped by the sample $h'_i = \partial \log H_i / \partial \log t$.

In some samples, distinguished as a rule by the large slope of the $J_c(H)_{H \rightarrow 0}$ plot, flux jumps were inevitably produced even when the external field was removed very slowly; these jumps reduced the frozen-in field H_i greatly. The measurements were performed in this case in a superconducting solenoid that produced a sufficiently stable external field $H < 50$ kOe. To plot $J_c(H)$ from the measured values of $\Delta H(H)$ we measured the values of $\langle J_c \rangle$ and $\langle H \rangle$ averaged over the sample thickness by a procedure similar to that described in Ref. 20.

RESULTS

Many properties, particularly the critical parameters of superconducting molybdenum sulfides $A_x\text{Mo}_6\text{S}_8$, are determined mainly by the element A. In addition, the critical parameters are strongly influenced by small deviations from stoichiometry and by the sample-preparation conditions; this manifests itself particularly strongly in superconducting molybdenum sulfides of the second group, the homogeneity region of which has not been distinctly established to this day. Thus, e.g., for molybdenum sulfides with lead the values of T_c and H_{c2} , according to the data of a number of studies,^{4,15,16,21} have a scatter that reaches 30 and 50%, respectively, while the densities of the critical current J_c can in this case differ by dozens of times. If we start with the formula PbMo_6S_8 then, as shown earlier,^{16,22} the maxima of the critical parameters are reached at a certain excess of molybdenum and lead. In this case, as follows from x-ray structure analysis

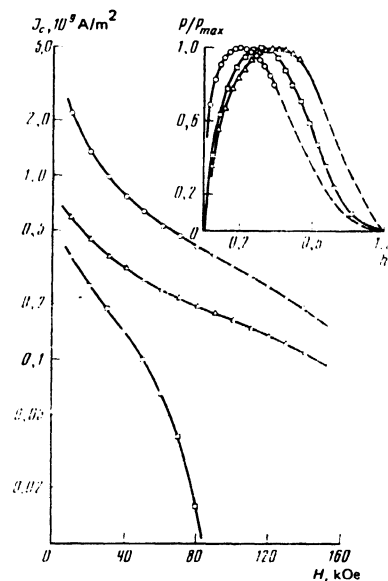


FIG. 3. Dependence of the critical-current density J_c on the applied magnetic field H at $T = 4.2$ K for the samples $\text{Pb}_{1.2}\text{Mo}_{6.4}\text{S}_8$ (\circ), $\text{Sn}_{1.2}\text{Mo}_{6.4}\text{S}_8$ (\triangle), $\text{Cu}_{1.8}\text{Mo}_6\text{S}_8$ (\square), annealed at the same temperature $T_a = 920^\circ\text{C}$. The inset shows the corresponding dependences of the normalized pinning force P/P_{max} on the relative magnetic field $h = H/H_{c2}^*$.

data, samples annealed at sufficiently high temperatures $T_a > 900^\circ\text{C}$ are practically single-phase.²³

Figure 3 shows the isotherms ($T = 4.2$ K) of the critical-current density as functions of the applied magnetic field for the samples $\text{Pb}_{1.2}\text{Mo}_{6.4}\text{S}_8$, $\text{Sn}_{1.2}\text{Mo}_{6.4}\text{S}_8$, and $\text{Cu}_{1.8}\text{Mo}_6\text{S}_8$, while the inset of Fig. 3 shows the corresponding plots of the pinning-force density, in relative coordinates P/P_{max} and $h = H/H_{c2}^*$, where H_{c2}^* is the magnetic field at which the sample resistivity is restored to the value $0.1 \rho_n$ at a current density 10^4 A/m^2 (ρ_n is the resistivity of the sample at $T = 15.5$ K). The samples were annealed at the same temperature $T_a = 920^\circ\text{C}$ for 24 h.

As seen from Fig. 3, the highest critical-current densities in the field interval from 10 to 140 kOe are observed for $\text{Pb}_{1.2}\text{Mo}_{6.4}\text{S}_8$ sample No. 3, which has also the maximum values of the remaining critical parameters: $T_c = 13.5$ K; $\partial H_{c2} / \partial T = 49$ kOe/K, and $H_{c2}(0) = 480$ kOe. The dependences of the pinning forces P , plotted in relative coordinates, are not similar, as seen from Fig. 2, and reach their maxima at different values $h = 0.2$, 0.33 , and 0.4 respectively for samples 3, 7, and 6.

Figure 4 shows the values of the pinning-force density $P(h)$ for a $\text{Cu}_{1.8}\text{Mo}_6\text{S}_8$ sample at fixed temperatures from 2 to 8 K. In the region of strong fields ($h > 0.25$) the experimental results can be approximated with sufficient accuracy by functions (solid lines in Fig. 4) of the form

$$P(T, h) = 9.25 P_{\text{max}}(T) h^{1/2} (1-h)^{1/2}, \quad (1)$$

where the plot of $P_{\text{max}}(T)$ at $T \geq 3$ K (see the inset of Fig. 4) is given by

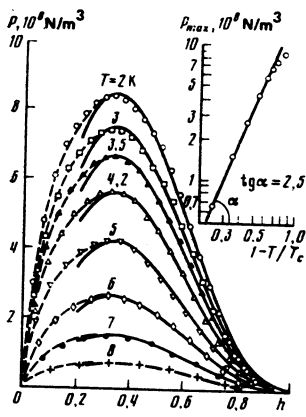


FIG. 4. Isotherms of the dependences of the pinning forces P on the relative magnetic field h for the sample $\text{Cu}_{1.8}\text{Mo}_6\text{S}_8$ at various temperatures. Inset—dependence of the maximum pinning-force density P_{max} on the temperature.

$$P_{\text{max}}(T) = P_0(1 - T/T_c)^{2.5}, \quad (2)$$

and $P_0 = 2 \times 10^9 \text{ N/m}^2$.

Similar plots of $P(h)$ with practically the same absolute values of $P_{\text{max}}(T)$ and with the same placements of the maxima near $h = 0.3$ were obtained earlier⁸ for thin-film $\text{Cu}_x\text{Mo}_6\text{S}_8$ samples.

In weak fields ($h < 0.3$) the experimental values of $P(T, h)$ satisfy sufficiently well the relation

$$P(T, h) = 1.33P_{\text{max}}(T)h(h + 0.1)^{-1}, \quad (3)$$

the plots of which are shown dashed in Fig. 4.

Equation (1), in which each of the factors depends only on one variable, T or h , is the mathematical form of the similarity law for the pinning forces, first formulated in 1969 by Fietz and Webb²⁴ on the basis of a study of the empirical data. Shortly after, however, considerable deviations from this law were observed,²⁵ and it was established that the similarity law describes the experimental data only if at least two basic requirements are satisfied: 1) the pinning mechanism is the same in the entire range of magnetic-fields and temperatures; 2) the magnetic field H in the sample exceeds substantially the first critical field H_{c1} .

It appears that at $H \gg H_{c1}$ this requirement is satisfied by the sample $\text{Cu}_{1.8}\text{Mo}_6\text{S}_8$. The role of the pinning centers in it can be played by microscopic inclusions of molybdenum disulfide and, possibly of free molybdenum, the number of which is at the limit of detection by x-ray diffraction.

A somewhat different situation is observed in the sample $\text{Pb}_{1.2}\text{Mo}_{6.4}\text{S}_8$. Indeed, at low temperatures $T < 5 \text{ K}$, as seen from Fig. 5, the similarity law is satisfied and the experimental values of $P(T, h)$ fit quite well plots (solid lines) of the form

$$P = 3.5P_{\text{max}}(T)h^{0.5}(1 - h)^2, \quad (4)$$

where the plot of $P_{\text{max}}(T)$ at $T \geq 2.4 \text{ K}$ (see the inset in Fig. 5) is described by the same expression (2) as in the

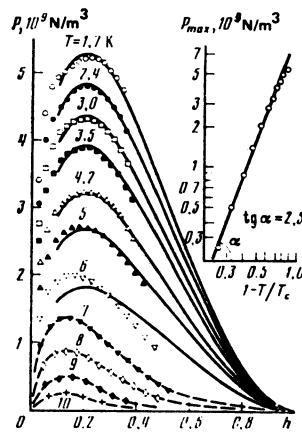


FIG. 5. Isotherms of the dependences of the density of the pinning forces P on the relative magnetic field h for the sample $\text{Pb}_{1.2}\text{Mo}_{6.4}\text{S}_8$ in the temperature range from 1.7 to 10 K. Inset—dependence of the maximum density of the pinning forces P_{max} on the temperature.

case of $\text{Cu}_{1.8}\text{Mo}_6\text{S}_8$, but with a different value of the constant, $P_0 = 9 \times 10^9 \text{ N/m}^2$. The relation (4) at constant T coincides with the theoretical expression for the pinning-force density obtained by Kramer²⁶ under the condition that the relative field h is strong enough.

With increasing temperature, starting with 5 K, the positions of the maxima on the isotherms of the pinning, force density, as seen from Fig. 5 begin to shift towards smaller values of h and expression (4) ceases to describe the experimental results. [A weak shift in the position of $P_{\text{max}}(h)$ with increasing temperature was observed earlier in an investigation of PbMo_6S_8 and $\text{Pb}_{1.5}\text{Mo}_{6.3}\text{S}_8$ samples.^{16,21}]

As seen from the presented data, the similarity law for the $\text{Pb}_{1.2}\text{Mo}_{6.4}\text{S}_8$ sample, which contains microscopic inclusions of several phases [Pb, PbS, MoS_2 , and Mo, Fig. 1] is satisfied only in a limited region $T < 5 \text{ K}$. It appears that failure to satisfy the similarity law in this case is due to the existence of several pinning

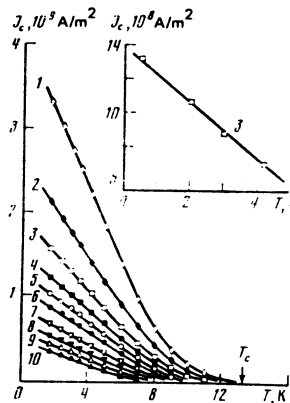


FIG. 6. Temperature dependences of the critical current density J_c form samples with composition $\text{Pb}_{1.2}\text{Mo}_{6.4}\text{S}_8$ annealed at $T_a = 920^\circ \text{ C}$ (in the inset, $T_a = 1020^\circ \text{ C}$), plotted at fixed values of the magnetic field (in kOe): 1—10, 2—20, 3—30, 4—40, 5—50, 6—60, 7—80, 8—100, 9—120, 10—140.

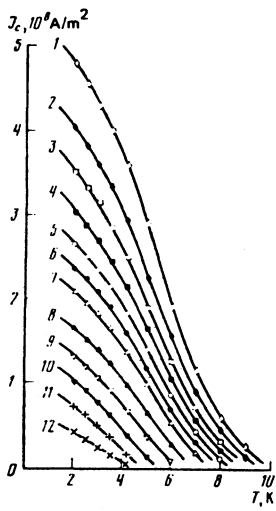


FIG. 7. Temperature dependences of the critical current density J_c for the sample $\text{Cu}_{1.8}\text{Mo}_6\text{S}_8$ ($T_a = 920^\circ\text{C}$), plotted at fixed values of the magnetic field H (in kOe): 1—10; 2—15; 3—20; 4—25; 5—30; 6—35; 7—40; 8—50; 9—60; 10—70; 11—80; 12—90.

mechanisms, whose effectiveness depends on the temperature.

The temperature dependences of the critical current density J_c , plotted at fixed values of the magnetic field for $\text{Pb}_{1.2}\text{Mo}_{6.4}\text{S}_8$, are shown in Fig. 6 and have, in contrast to analogous plots for $\text{Cu}_{1.8}\text{Mo}_6\text{S}_8$ (Fig. 7), extended linear sections in the temperature region from 1.7 to 7 K. Measurements of J_c at lower temperatures for $\text{Pb}_{1.2}\text{Mo}_{6.4}\text{S}_8$ sample No. 3 ($T_a = 920^\circ\text{C}$) could not be performed because of the jumps in the flux and the insufficient field strength $H = 50$ kOe in the facility with helium-3. These measurements were therefore performed on sample No. 4 (see Table I) having the same composition, but annealed at a higher temperature $T_a = 1020^\circ\text{C}$, in which the probability of flux jumps was much lower.

As seen from the inset in Fig. 6, at low temperatures the $J_c(T)$ plot for sample No. 4 remains linear down to the lowest values $T = 0.5$ K.

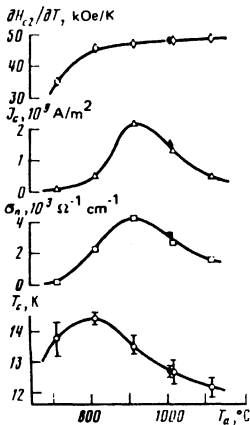


FIG. 8. Variation of the critical parameters $\partial H_{c2}/\partial T$, J_c ($H = 10$ kOe, $T = 4.2$ K), T_c , and of the conductivity σ_n of samples of the system $\text{Pb}_{1.2}\text{Mo}_{6.4}\text{S}_8$ as functions of the annealing temperature T_a .

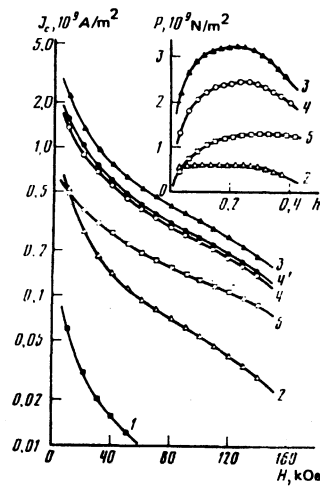


FIG. 9. Isotherms ($T = 4.2$ K) of the dependences of the critical-current density J_c and of the density J_c and of the density of the pinning forces P (in the inset) for samples of the $\text{Pb}_{1.2}\text{Mo}_{6.4}\text{S}_8$ system annealed at various temperatures (in $^\circ\text{C}$): 1—720; 2—820, 3—920, 4—1000; 4—1020, 5—1120.

The influence of the annealing temperature T_a on the critical parameters and the conductivity σ_n of the samples of the system $\text{Pb}_{1.2}\text{Mo}_{6.4}\text{S}_8$ is shown in Fig. 8. The vertical segments on the $T_c(T_a)$ plot denote the width ΔT , of the transition into the superconducting state and correspond to a change of the resistivity of the samples from $0.1\rho_n$ to $0.9\rho_n$. The conductivity σ_n of the samples in the normal state, was measured at the same temperature 15.5 K. The values of J_c corresponded to a field 10 kOe and a temperature 4.2 K. The derivative $\partial H_{c2}/\partial T$ was determined from the slope of the linear section on the $H_{c2}(T)$ plot in the field interval from 20 to 140 kOe.

To illustrate the reproducibility of the results, Fig. 8 shows data for two samples, 4' and 4, which have close values of T_a , 1000 and 1020 $^\circ\text{C}$ respectively.

The maximum value $T_c = 14.4$ K and the narrowest transition $\Delta T = 0.3$ K were observed for sample 2, annealed at 820 $^\circ\text{C}$. An increase of T_a by 100 $^\circ\text{C}$ lowers T_c by 0.9 K and increases J_c (4.2 K; 10 kOe) by 4.4 times. Figure 9 shows the isotherms of $J_c(H)$, plotted at 4.2 K for $\text{Pb}_{1.2}\text{Mo}_{6.4}\text{S}_8$ samples with different annealing temperatures from 720 to 1120 $^\circ\text{C}$. It is seen that with increasing T_a the plots of $J_c(H)$ become less steep, and the maximum density of the pinning forces shifts towards larger values of the relative field h .

Figure 10 shows the time variation of the internal field in samples 2–5. The measurements were made in the absence of an external field at $T = 4.2$ K. Except for a small initial section ($t < 20$ sec), the relative change of the internal field $H_i(t)/H_i(5)$, as seen from Fig. 10, is well described by a logarithmic law, where $H_i(5)$ is the value of the field "frozen" in the sample at 5 seconds after turning off the current in the Bitter solenoid. The $H_i(t)$ dependences were not measured for sample 1 because of the small value of $H_i(5)$. The values of $H_i(5)$ for samples 1–7 at $T = 4.2$ K are listed in Table II. The frozen-in field decreases most rapidly in sample 5, which x-ray diffraction analy-

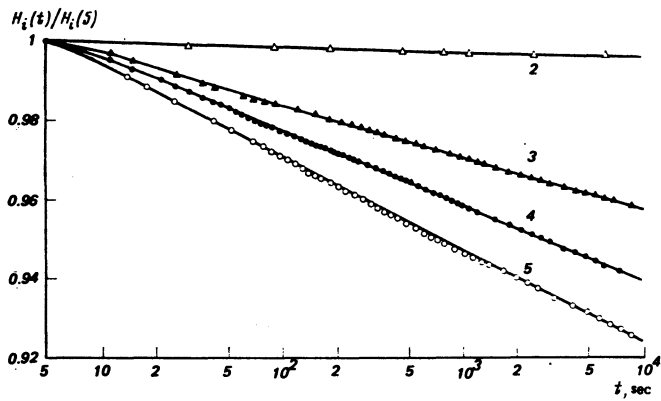


FIG. 10. Relative time dependence of the field H_1 "frozen" in the samples. The numbers next to the lines denote the numbers of the samples in accordance with Table I.

sis shows to contain practically no extraneous phases (see Fig. 1).

If $H_1(t)/H_1(5)$ is extrapolated towards larger values of t , it becomes possible to estimate the time $t_{1/2}$ (see Table II) during which the current in the sample would decrease to one-half.

DISCUSSION OF RESULTS

As already noted earlier,^{4,27} ternary molybdenum chalcogenides are type-II superconductors. Some of them are characterized by very large values of the Ginzburg-Landau parameter, $\kappa > 50$, and a small mean free path, $l = 20-30 \text{ \AA}$. Since $H_{c2} \sim \Phi_0/\xi_0 l$ and $J_c \sim (l/\xi_0)^{1/2}$ (Ref. 28) at $l \ll \xi_0$ (ξ_0 is the correlation length and Φ_0 is the flux quantum), one might expect compounds with extremely high values of H_{c2} , such as $\text{Pb}_x\text{Mo}_6\text{S}_8$, to have a low critical current density. However, even the first studies^{5,6,9} devoted to this question have shown that the critical current density of ternary and four-component molybdenum sulfides is high enough and approaches in a number of cases the values of J_c obtained for the better samples of Nb_3Sn and Nb_3Ge . If it is assumed that J_c in the Chevrel phases depends principally on the microstructure of the samples, the analysis of the current characteristics of the molybdenum sulfides can be carried out in this case on the basis of the ordinary premises for type-II superconductors. Such an analysis, as will be shown below, does not lead to any contradiction with the experimental data, and from this point of view is perfectly justified although it may call for a more rigorous corroboration.

TABLE II. Parameters of superconducting state of ternary molybdenum sulfides.

Sample No.	T_c , K	$H_{c2}(\theta)$, kOe	$J_c(10 \text{ kOe})$, 10^9 A/m^2	$J_c(100 \text{ kOe})$, 10^9 A/m^2	$J_c(10 \text{ kOe})$, 10^9 A/m^2	$P(0)$, 10^9 N/m^2	P_{max} , 10^9 N/m^2	B_{c1} , T	$H_{c2}(\theta)$, kOe	$t_{1/2}$, years	d_B , \AA	d_L , \AA
1	13.8	360	0.06	—	—	0.06	0.06	0.05	2	—	2000	—
2	14.4	500	0.52	0.53	9.8	0.6	0.56	0.2	11	10^{20}	970	650
3	13.5	480	2.20	3.20	6.9	3.6	3.20	0.7	25	10^{21}	530	220
4	12.7	460	1.35	2.30	5.9	2.7	2.33	1.0	18	10^{21}	440	230
5	12.2	450	0.49	1.27	3.9	1.55	1.27	2.1	9	10^{21}	310	250
6	12.7	370	0.58	1.60	3.6	2.05	1.60	2.5	14	10^{22}	280	220
7	10.9	160	0.36	—	—	0.76	0.56	1.1	9	10^{23}	430	410

It is known that high critical-current densities in type-II superconductors are usually due to the presence of defects in their crystal lattice, which hinder the free motion of the vortex filaments (fluxoids), making the magnetization curves irreversible. Conversely, in type-II superconductors which have almost reversible magnetization curves, the critical current is very small.²⁹

The interaction of the fluxoids with the defects (pinning) prevents a jumplike change of the magnetic flux in the sample at $H \geq H_{c1}$. Likewise, when the external field decreases from a value $H > H_{c1}$, the flux turns out to be trapped in the sample. In both cases the pinning produces a nonequilibrium distribution of the fluxoids and consequently a magnetic field gradient whose presence indicates that current directed perpendicular to the sample axis circulates in the sample. As proposed in Bean's model,³ in each region of the sample there flows the maximum possible current, whose value naturally must not exceed the pair-breaking current.^{28,31}

Although experimental and theoretical investigations of pinning have been the subject of many studies, there is still no full understanding of the mechanism of this phenomenon even in those cases when the metallurgical features of the superconductors are well known.

Nonetheless, it can be assumed even now that the maximum of the pinning forces P_{max} is reached if each fluxoid interacts with an individual microdefect, whose dimension in a direction perpendicular to the applied field should be close to the coherence length ξ .

At the optimal distribution of the pinning centers in the superconducting matrix, the maximum density of the transverse critical current, according to recent (1980) calculations by Brandt,³² is

$$J_{c \text{ max}} \approx [H_{c2}(T) - H] / 2 \kappa \xi(T) \quad (5)$$

Using Goodman's³² equation for κ we obtain from (5)

$$J_{c \text{ max}} \approx \sigma_n \xi(T) \frac{H_{c2}(T) - H}{2.06 \cdot 10^4 \xi_0^2} \left(- \frac{\partial H_{c2}}{\partial T} \right)^{-1}, \quad (6)$$

where

$$\sigma_n = 1/\rho_n \text{ (}\Omega^{-1} \text{ cm}^{-1}\text{)}, \quad \xi(T) = (\Phi_0/2\pi H_{c2})^{1/2} \text{ (cm)}, \quad H_{c2} \text{ (Oe)}, \quad J_c \text{ (A/cm}^2\text{)}.$$

For molybdenum sulfide with lead, estimates in accord with Eqs. (5) and (6) yield $J_{c \text{ max}} = 2.5 \times 10^{10} \text{ A/m}^2$ in a field 10 kOe and at $T = 4.2 \text{ K}$. This is somewhat higher than the $J_{c \text{ max}}$ estimated^{8,34} for PbMo_6S_8 from somewhat different considerations, and exceeds by approximately one order the corresponding value of J_c for sample 3.

Relation (6) explains also the correlation observed earlier¹⁶ and in the present study (see Fig. 8) between the values of J_c and σ_n . The difference between the temperature dependences of J_c for molybdenum sulfides with lead (Fig. 6) and with copper (Fig. 7) at low temperatures ($T < 5 \text{ K}$), where the similarity law holds for both compounds, can be explained within the framework of Kramer's theory²⁶:

$$J_c(T) = A [H_{c2}(T) - H]^{1/2} / H_{c2}^{3/2} \kappa^2(T), \quad (7)$$

where A is a constant.

It follows from the data of Refs. 3 and 35 that the experimental values of $H_{c2}(T)$ for ternary molybdenum sulfides with lead and with copper are well approximated by the expression

$$H_{c2}(T) = H_{c2}(0) [1 - (T/T_c)^2]. \quad (8)$$

An analysis of (7) with account taken of (8) shows that the positive curvature of the plots of $J_c(T)$ for $\text{Cu}_{1.8}\text{Mo}_6\text{S}_8$ and the practically linear increase of J_c of $\text{Pb}_{1.2}\text{Mo}_{6.4}\text{S}_8$ are due most likely to the difference between the temperature dependences of the parameter $\kappa_1(T)$ of these compounds. Such a difference in the behavior of $\kappa_1(T)$ can set in, e.g., because of the different values of the electron mean free path in compounds with lead and with copper, and the path should be larger in the latter. This conclusion agrees with the measurements of the temperature dependence of the resistivity of $\text{Cu}_{1.8}\text{Mo}_6\text{S}_8$ ($\rho_{300}/\rho_n = 11$; $\mu_n = 1.2 \cdot 10^{-1} \Omega\text{-cm}$) and $\text{Pb}_{1.2}\text{Mo}_{6.4}\text{S}_8$ ($\rho_{300}/\rho_n = 2.2$; $\rho_n = 2.3 \cdot 10^{-4} \Omega\text{-cm}$). However, Gelfand and Werthamer³⁶ have shown in their calculations that as $T \rightarrow 0$ $\kappa_1(T)$ depends very little on l , meaning that the difference in the character of the $J_c(T)$ curves of the compounds $\text{Cu}_{1.8}\text{Mo}_6\text{S}_8$ and $\text{Pb}_{1.2}\text{Mo}_6\text{S}_8$ is also small.

The effect of different factors on $\kappa_1(T)$ was investigated by Eilenberger,³⁷ who has shown that the temperature dependence of the parameter $\kappa_1(T \rightarrow 0)$ is strongly influenced by the electron-scattering anisotropy l_t/l (l_t is the transport mean free path).

From this point of view, good agreement between experiment and theory²⁶ will be reached if it is assumed that there is practically no electron-scattering anisotropy in $\text{Cu}_{1.8}\text{Mo}_6\text{S}_8$ ($l_t/l \approx 1$), while $l_t/l \approx 1.5$ for $\text{Pb}_{1.2}\text{Mo}_{6.4}\text{S}_8$. Analogous conclusions can be arrived also on the basis of an analysis of expression (5), if the parameter κ is replaced in it by $\kappa_1(T)$.

As first shown in the experiments of Kim *et al.*,²⁰ the internal field in type-II superconductors in the form of hollow cylinders attenuates logarithmically with time. An analogous behavior of $H_i(t)$ at $t > 20$ sec is observed also in investigations of samples of molybdenum sulfides in our experiments. The rate of change of $H_i(t)$ is very strongly influenced, as seen from Fig. 10, by the sample annealing temperature, with the rate of change of the internal field $h'_i = \partial \log H_i / \partial \log t$ increasing with increasing T_a . Among the molybdenum sulfides with the same value of $T_a = 920^\circ\text{C}$, the slowest to decrease at $T = 4.2$ K is the frozen-in field of the compound $\text{Cu}_{1.8}\text{Mo}_6\text{S}_8$ ($t_{1/2} = 10^{93}$ years), followed by $\text{Pb}_{1.2}\text{Mo}_{6.4}\text{S}_8$ ($t_{1/2} = 10^{31}$ years) and $\text{Sn}_{1.2}\text{Mo}_{6.4}\text{S}_8$ ($t_{1/2} = 10^{22}$ years).

The first to explain the logarithmic variation of the field (the creep of the flux) was Anderson.³⁸ In addition, his theory, based on classical analysis of the activation mechanism relative to the fluxoid beams, has explained also the strong temperature dependence of J_c observed in the low-temperature region $0.1 < T/T_c < 0.5$ in experiments on type-II superconductors.

The relative change of the field in hollow cylindrical superconductors with wall thickness w is given, according to Anderson's theory, by

$$\frac{\delta H_i}{H_i} = - \frac{k'w}{H_i(H_i + B_0/\mu_0)} \frac{kT}{d_i} \ln t, \quad (9)$$

where $k' = 0.4\pi$; $B_0 = \Phi_0/d_B^2$, d_i is the average dimension of the fluxoid beam in centimeters and depends on the sizes of the microinclusions and on the distances between them.

For all the investigated samples, the experimental values of $J_c(H)$ in the field region up to 70 kOe at constant T can be approximated with sufficient accuracy by expressions of the type

$$J_c(H) = P(0)/(\mu_0 H + B_0), \quad (10)$$

where $P(0)$ and B_0 are characteristic constants of the superconductor. The values of these constants, as well as the average dimensions d_B of the fluxoid beams calculated from B_0 , are given in Table II.

With increasing annealing temperature, as already noted, the samples become more single-phase, and the large defects and inclusions of other phases decrease and break up into several smaller ones. (The increase in the number of pinning centers with increasing T_a is evidenced by the increase of B_0 .) Starting with $T_a = 920^\circ\text{C}$, the decrease in the sizes of the pinning centers is no longer offset by the increase of the number, while the density of the pinning forces decreases in the field region $h < 0.5$ (see the inset of Fig. 9).

If it is assumed that in sample 5 the average size of the pinning centers is much less than the average distance between them and is approximately equal to the coherence length $\xi = 20\text{--}22 \text{ \AA}$, then the optimal value $d_0 = \xi(6/h)^{1/2}$ for the relative field $h = 0.5$ (Ref. 31) would in this case be $70\text{--}77 \text{ \AA}$, which is one-quarter the value of d_B calculated from B_0 . Thus, at the optimal distribution of the pinning centers one might expect the density of the critical current in the $\text{Pb}_{1.2}\text{Mo}_{6.4}\text{S}_8$ system to be several times larger than the reached value of J_c .

Measurements of the temperature dependence of the relative damping rate $h'_i = \partial \log H_i / \partial \log t$ in the temperature range from 0.5 to 4.2 K have shown that h'_i decreases much less with temperature than would follow from Anderson's theory, which does not take into account, e.g., the possibility of quantum tunneling of fluxoid beams or of individual fluxoids through the energy barriers that separate neighboring pinning centers.

CONCLUSION

The features of the superconducting state of bulk samples of the highest-temperature ternary sulfides of molybdenum of the first and second groups were investigated in a wide range of magnetic fields and temperatures. Among the ternary molybdenum sulfides prepared under identical technological conditions, the maximum values of all three critical parameters T_c , H_{c2} , and J_c are possessed by compounds with lead.

It was shown that for molybdenum sulfides with copper the similarity law holds in the entire range of investigated temperatures from 2 to 8 K, whereas for the compound $\text{Pb}_{1.2}\text{Mo}_{6.4}\text{S}_8$ it is valid only in the limited region $T < 5$ K.

The presence of positive curvature in the plot of $J_c(T, H = \text{const})$ at low temperatures for $\text{Cu}_{1.8}\text{Mo}_6\text{S}_8$, and the practically linear plot of $J_c(T, H = \text{const})$ in the temperature range from 0.5 to 6 K for $\text{Pb}_{1.2}\text{Mo}_{6.4}\text{S}_8$ can be attributed to the difference in the mean free paths and the singularities of the scattering of the electrons in these systems.

The influence of the annealing temperature T_a on J_c and on other parameters of these compounds were investigated with $\text{Pb}_{1.2}\text{Mo}_{6.4}\text{S}_8$ as the example.

The connection between the shape of the $J_c(H, T = \text{const})$ curves and the damping rate of the critical current in the samples was analyzed. It was observed that for all the investigated samples the rate of damping of J_c decreases with decreasing temperature much more slowly than called for by Anderson's theory. The maximum critical current density J_c (140 kOe; 1.7 K) = 3.5×10^8 A/m² is observed for a $\text{Pb}_{1.2}\text{Mo}_{6.4}\text{S}_8$ sample annealed at $T_a = 920^\circ\text{C}$.

An analysis of the results gives all grounds for stating that the critical parameters are reached by now in this class of compounds are not their limits and further research is needed not only to refine the physical picture of the superconductivity in molybdenum sulfides but also to estimate more fully the prospect of their practical use.

¹⁾Owing to the very little values of the first critical field, $H_{c1} < 1$ kOe, and to the absence of ferromagnetic inclusions in the investigated compounds, it can be assumed that at $H \gg H_{c1}$ we have $\langle B \rangle = \mu_0 H$, where $\langle B \rangle$ is the induction in the sample, averaged over distances exceeding the coherence length ξ .

¹S. M. Foner, E. J. McNiff, Jr., and E. J. Alexander, Phys. Lett. **49A**, 269 (1974).

²Ø. Fischer, M. Decroux, S. Roth, R. Chevrel, and M. Sergent, J. Phys. **C8**, L474 (1975).

³N. E. Alekseevskii, A. V. Mitin, C. Bazan, N. M. Dobrovol'skii, and B. Rachka, Zh. Eksp. Teor. Fiz. **74**, 384 (1978) [Sov. Phys. JETP **47**, 199 (1978)].

⁴Ø. Fischer, Appl. Phys. **16**, 1 (1978).

⁵N. E. Alekseevskii, M. Glinski, N. M. Dobrovol'skii, and V. I. Tsebro, Pis'ma Zh. Eksp. Teor. Fiz. **23**, 455 (1976) [JETP Lett. **23**, 412 (1976)].

⁶N. E. Alekseevskii, N. M. Dobrovol'skii, D. Eckert, and V. I. Tsebro, Zh. Eksp. Teor. Fiz. **72**, 1145 (1977) [Sov. Phys. JETP **45**, 599 (1977)].

JETP **45**, 599 (1977)].

⁷N. E. Alekseevskii, N. M. Dobrovol'skii, D. Eckert, and V. I. Tsebro, J. Low Temp. Phys. **29**, 565 (1977).

⁸S. A. Alterovitz, J. A. Woollam, L. Makkerdiner, and Huey-Lin Luo, J. Low Temp. Phys. **30**, 797 (1978).

⁹M. Decroux, Ø. Fischer, and R. Chevrel, Cryogenics **17**, 291 (1977).

¹⁰T. Luhman and D. Dew-Hughes, J. Appl. Phys. **49**, 936 (1978).

¹¹S. A. Alterovitz, J. A. Woollam, L. Kammerdiner, and Huey-Lin Luo, Appl. Phys. Lett. **33**, 264 (1978).

¹²V. A. Lykhin, V. S. Kruglov, Yu. N. Likhinin, and A. S. Nigmatulin, Pis'ma Zh. Tekh. Fiz. **6**, 168 (1980) [Sov. Tech. Phys. Lett. **6**, 74 (1980)].

¹³C. Rossel, B. Seeber, and Ø. Fischer, Phys. Stat. Sol. (a) **59**, K43 (1980).

¹⁴P. Przyslupski, R. Horyń, and B. Greń, J. Low Temp. Phys. **38**, 93 (1980).

¹⁵N. E. Alekseevskii, A. V. Mitin, and C. Bazan, Dokl. Akad. Nauk SSSR **245**, 358 (1979) [Sov. Phys. Dokl. **24**, 212 (1979)].

¹⁶N. E. Alekseevskii and A. V. Mitin, Fiz. Met. Metallov. **50**, 1179 (1980).

¹⁷N. E. Alekseevskii, Zh. Eksp. Teor. Fiz. **8**, 1098 (1938).

¹⁸D. Eckert and A. Handstein, Phys. Stat. Sol. (a), **37**, 171 (1976).

¹⁹L. J. Heuringer and Y. Shapira, Rev. Sci. Instrum. **10**, 1314 (1969).

²⁰Y. B. Kim, C. F. Hempstead, and A. R. Strnad, Phys. Rev. Lett. **9**, 306 (1962).

²¹S. A. Alterovitz and J. A. Woollam, Phil. Mag. **B 38**, 619 (1978).

²²S. Foner, E. J. McNiff, Jr., and E. J. Alexander, IEEE Trans. Magn. **11**, 155 (1975).

²³J. Hauck, Math. Res. Bull. **12**, 1015 (1977).

²⁴W. A. Fietz and W. W. Webb, Phys. Rev. **178**, 657 (1969).

²⁵O. Béthoux and J. Y. Guerin, Proc. 12-th Intern. Conf. on Low Temp. Phys., LT12, E. Kanda, ed., Academic Press of Japan, 1971, p. 379.

²⁶E. J. Kramer, J. Electronic Mat. **4**, 839 (1975).

²⁷N. E. Alekseevskii, Cryogenics **20**, 257 (1980).

²⁸K. Maki, Progr. Theor. Phys. **29**, 10 (1963).

²⁹J. D. Livingston, Phys. Rev. **129**, 1943 (1963).

³⁰C. P. Bean, Phys. Rev. Lett. **8**, 250 (1962).

³¹R. G. Boyd, Phys. Rev. **145**, 255 (1966).

³²E. H. Brandt, Phys. Lett. **77A**, 484 (1980).

³³V. V. Goodman, IBM J. Res. Dev. **6**, 63 (1962).

³⁴S. A. Alterovitz and J. A. Woollam, Cryogenics **19**, 167 (1979).

³⁵S. A. Alterovitz and J. A. Woollam, Sol. St. Commun. **25**, 141 (1978).

³⁶E. Helfand and N. R. Werthamer, Phys. Rev. **147**, 288 (1966).

³⁷G. Eilenberger, Phys. Rev. **153**, 584 (1967).

³⁸P. W. Anderson, Phys. Rev. Lett. **9**, 309 (1962).

Translated by J. G. Adashko